

Elasticity and Viscosity of a Lyotropic Chromonic Nematic Studied with Dynamic Light Scattering.

Yu. A. Nastishin^{1,2}, K. Neupane³, A. R. Baldwin³, O. D. Lavrentovich^{1,4,*} and S. Sprunt^{3†}

¹ *Liquid Crystal Institute, Kent State University, POB 5190, Kent, OH 44242*

² *Institute of Physical Optics, 23 Dragomanov str., Lviv, 79005, Ukraine*

³ *Department of Physics, Kent State University, Kent, OH, 44242*

⁴ *Chemical Physics Interdisciplinary Program, Kent State University, Kent, OH 44242*

(Dated: November 2, 2018)

Using dynamic light scattering, we measure for the first time the temperature-dependent elastic moduli and associated orientational viscosity coefficients of the nematic phase in a self-assembled lyotropic chromonic liquid crystal. The bend K_3 and splay K_1 moduli are an order of magnitude higher than the twist K_2 constant. The ratio K_3/K_1 shows an anomalous increase with temperature; we attribute this to the shortening of the aggregates as temperature increases. The viscosity coefficients also show a significant anisotropy, as well as a strong temperature dependence; in particular, the bend viscosity is three orders of magnitude smaller than the splay and twist viscosities.

PACS numbers: 61.30.-v, 61.30.Eb, 61.30.St, 64.75.Yz, 78.35.+c

Molecular self-assembly in solutions often results in anisometric aggregates capable of orientational order. The simplest examples are end-to-end “living polymerization”, formation of worm micelles by surfactants, and face-to-face chromonic assembly of disc-like molecules into stacks [1, 2, 3]. In many systems, ranging from organic dyes and drugs [1] to DNA [4], this mostly one-dimensional aggregation produces a broadly polydisperse system of “building units” that form nematic or columnar phases and are generally classified as lyotropic chromonic liquid crystals (LCLCs). The structural organization and properties of LCLCs should depend on the properties of both the individual molecules and their aggregates. Since the length of the aggregates is not fixed by covalent bonds, it is expected to vary strongly with concentration, temperature, ionic content, etc., making the LCLCs very different from the classic liquid crystals in which the building units are individual molecules of fixed shape. Despite the growing interest in the LCLCs [1, 4], very little is known about their molecular structure and practically nothing is known about their elastic and viscous properties.

In this paper, we use dynamic light scattering from orientational fluctuations to determine experimentally the fundamental elastic and viscous properties of a nematic LCLC, following the approach developed by Meyer’s group for lyotropic polymer nematics [5]. In particular, we study 14wt% solutions of Disodium Cromoglycate (DSCG) purchased from Spectrum Chemicals, 98% purity, in deionized water (initial resistivity 18 $M\Omega cm$). The homogeneous nematic phase is stable up to the temperature $T_{NI} \approx 301$ K, above which the mixture is in the biphasic nematic - isotropic state. Our experiment was facilitated by the recent development of aligning techniques for LCLCs [6] - specifically, the flat glass substrates used to sandwich 16 μm thick samples were coated with a buffed layer of the SE-7511 polymer (Nis-

san Chemical Inc.) for uniform planar orientation of the director \vec{n} [6]. The cells were carefully sealed with epoxy to prevent water evaporation. To mitigate possible effects of sample aging, we allowed the cells to equilibrate for 48 hours; subsequent measurements were completed within 15 hours. Longer equilibration worsens alignment, causing parasitic static scattering. The sample temperature was controlled within 0.1 $^\circ C$ by a hot stage (Instec). Light of wavelength $\lambda = 532$ nm from a diode-pumped solid state laser (Coherent, model Verdi V8) was focused (beam waist 50 μm) normally onto the sample. The incident light polarization was vertical; the analyzer direction and the scattering plane were both horizontal.

In the two studied geometries the nematic director \vec{n} is either (1) perpendicular (splay + twist geometry) or (2) parallel (bend-twist geometry) to the scattering plane. Homodyne cross-correlation functions of the scattered light intensity (evenly split between two independent detectors) were recorded as a function of time on a nanosecond digital correlator. In geometry (1), two overdamped relaxation modes: splay [amplitude A_1 , relaxation rate Γ_1] and twist [A_2, Γ_2] are expected [7]. As determined by standard selection rules for nematic light scattering, the faster mode corresponds to the splay director deformation, and the slower mode assigns to the twist deformation. Typical time correlation data are shown on the right side in Fig.1. Double exponential fitting of the decay of bend-twist fluctuations for geometry (2), displayed on the left in Fig.1, combined with an alternative analysis by the regularization method (see figure inset) [8], results in an additional two modes with distinctive relaxation rates Γ_3 and Γ_4 and corresponding amplitudes A_3 and A_4 . The best single-exponential fit, shown by the thin line in Fig.1, does not match the slower portion of the decay. The faster, more intense mode [A_3, Γ_3] is assigned to bend-twist fluctuations, which are expected to dominate the depolarized scattering when \vec{n} lies in the

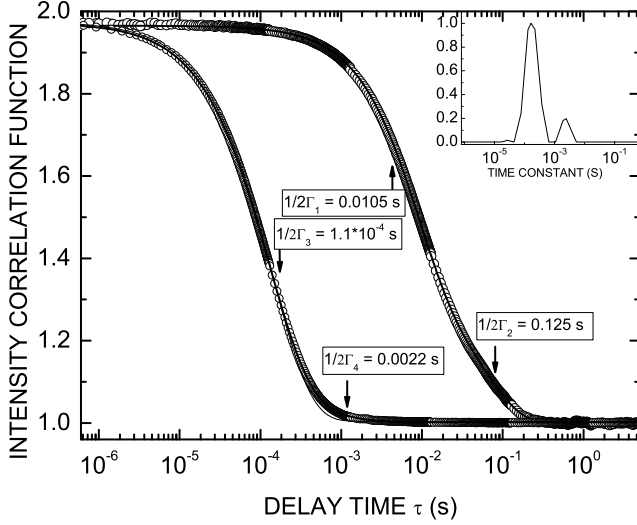


FIG. 1: Correlation functions (open circles) collected at $T = 294 \text{ C}$ for $q = 1.64 \times 10^6 \text{ m}^{-1}$ in a predominantly bend (left) and for $q = 1.00 \times 10^7 \text{ m}^{-1}$ in splay + twist geometries (right). Double-exponential fits (thick lines) of the correlation functions give respectively: amplitude and relaxation rate of splay $[A_1, \Gamma_1]$, twist $[A_2, \Gamma_2]$, bend $[A_3, \Gamma_3]$, and an additional $[A_4, \Gamma_4]$ mode. The thin line for the bend correlation function (left) represents a best single-exponential fit, which is clearly inadequate. Inset shows the relaxation time spectrum obtained by the regularization method [8] for the bend geometry correlation function; the small secondary peak confirms the presence of the additional mode $[A_4, \Gamma_4]$.

scattering plane. The weaker mode $[A_4, \Gamma_4]$ cannot be attributed to a simple leakage of splay or twist fluctuations potentially due to slight errors in setting geometry (2), as Γ_4 substantially exceeds both Γ_1 and Γ_2 , even when the latter two are measured at an order of magnitude larger wavenumber q . In this context, we observe from Fig. 2 that all detected modes are hydrodynamic ($\Gamma \sim q^2$), as is normally expected for orientational fluctuations.

For normally incident light, the amplitude and relaxation rate of the bend-twist mode scale as $A_3 \sim (K_2 q_{\perp}^2 + K_3 q_{\parallel}^2)^{-1}$ and $\Gamma_3 \sim K_2 q_{\perp}^2 + K_3 q_{\parallel}^2$ [7]. (Here \parallel means along \vec{n} .) For small scattering angles, one has $K_2 q_{\perp}^2 \ll K_3 q_{\parallel}^2$. Assuming for the moment $K_2 \approx K_3$, the ratio of these two terms is $(\sin \theta_b)^2 / 4n^2$, which ranges from ≈ 0.01 for the lowest scattering angle ($\theta_b = 15^\circ$) to 0.1 for the largest (65°). Here n is the refractive index of the solution. In fact, as shown below, $K_3 \approx (30 - 40)K_2$, and thus the contribution of $K_2 q_{\perp}^2$ to the amplitude and relaxation rate of the mode $[A_3, \Gamma_3]$ is utterly negligible over the whole angular range studied. Therefore, the dispersion of bend fluctuations can be accurately measured while keeping the incident light normal to the sample substrates, thus avoiding rotation of the sample in a q -scan and potential problems associated with slight non-

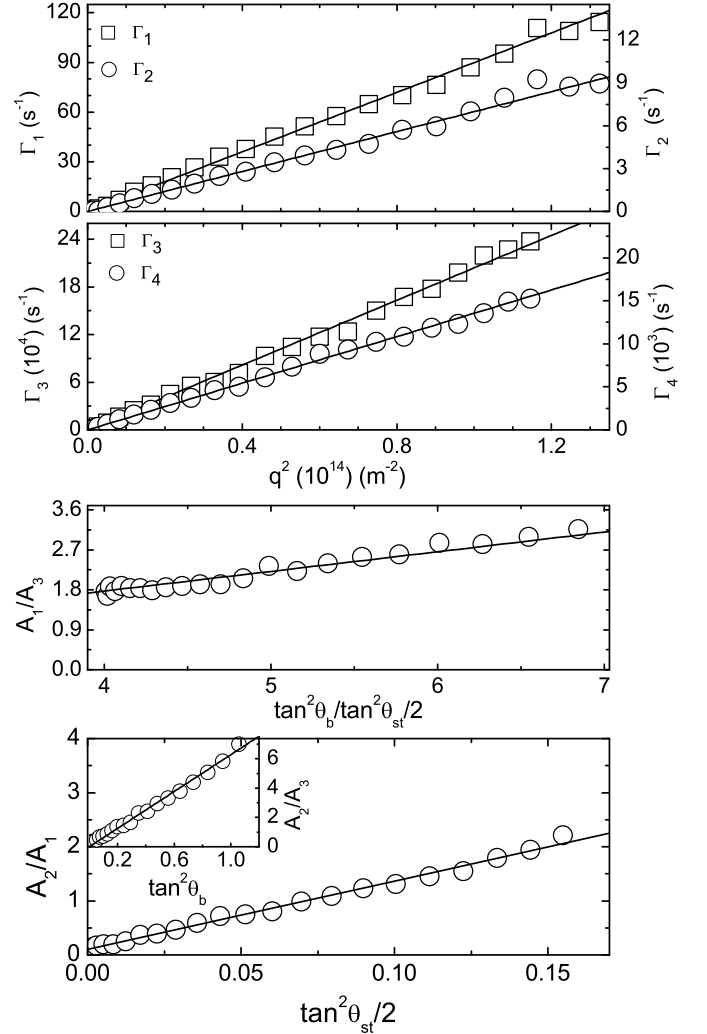


FIG. 2: Angular dependencies of the rates and ratios of the amplitudes of the relaxation modes. Solid lines represent fits described in the text.

uniformity of alignment.

The variation of the relaxation rates and the amplitude ratios with scattering wavenumber q or scattering angle θ for the director modes follows the expected behavior (solid lines in Fig. 2): $\Gamma_i = \frac{K_i}{\eta_i} q^2$; $\frac{A_2}{A_1} = \frac{K_1}{K_2} \tan^2 \frac{\theta_{st}}{2}$, $\frac{A_2}{A_3} = \frac{K_3}{4K_2} \tan^2 \theta_b$ and $\frac{A_1}{A_3} = \frac{K_3}{4K_1} \frac{\tan^2 \theta_b}{\tan^2 \frac{\theta_{st}}{2}}$, where η_i with $i = 1, 2, 3$ stand for viscosities corresponding to splay, twist and bend deformations, respectively. Since the refractive index anisotropy $\Delta n = 0.02$ is small [6], one has $q = \frac{4\pi}{\lambda} n \sin \frac{\theta_{st}}{2}$ or $q = \frac{2\pi}{\lambda} n \sin \theta_b$, where θ_{st} and θ_b are the scattering angles, in the splay+twist and bend geometries, respectively. Good fitting of the relaxation rates and the amplitudes indicates that data collected during the experiment are not significantly affected by sample aging.

From data for the amplitudes measured on heating at

fixed scattering angles ($\theta_{st} = 40^\circ$ for splay+twist and $\theta_b = 15^\circ$ for bend geometries, respectively) we deduced the temperature dependencies of the elastic moduli ratios (Fig. 3 a). Absolute values of the moduli (Fig. 3 b) were determined by calibrating the scattered intensity against an identical cell filled with the standard thermotropic nematic (4'-n-pentyl-4-cyanobiphenyl, 5CB) for a pure bend geometry at 294 K. We then used the known $K_3 = 18$ pN, $\Delta n = 0.201$ for 5CB [9], and the temperature dependence of Δn for our chromonematic [6], to obtain $K_3 = 28$ pN at 294 K. Finally we combined the results for the elasticities with data for the relaxation rates to find the associated orientational viscosities (Fig. 3e).

Within the phenomenological Landau-de Gennes theory, it is expected that the temperature behavior of $K_i \sim S^2$ and $\Delta n \sim S$ are determined by the temperature dependency of the scalar order parameter S [7]. In the chromonematic case, we find that only the twist mode follows this expectation, as the amplitude $A_2 \sim \frac{(\Delta n)^2}{K_2}$ is temperature independent [7] (Fig. 3 c). In contrast, $K_3/(\Delta n)^2$ and $K_1/(\Delta n)^2$ both decrease as temperature increases. The effect can be qualitatively explained by shortening of aggregates with increasing T [10], which should affect K_1 and K_3 , but not significantly K_2 [11]. Meyer [3] predicted that in a self-assembled chromonematic, $K_1 = \frac{k_B T}{4d} \frac{L}{d}$, where $L = L_0 \exp \frac{E_a}{2k_B T}$ is the average aggregate length [2], L_0 is a constant, E_a is the scission energy needed to split an aggregate into two, k_B is the Boltzmann constant, and d is the diameter of the stack. Qualitatively, Meyer's model describes the data well (Fig. 3 d). It is of interest to explore whether the fitting parameters are close to the physical expectations.

For the analysis, we consider $K_1/K_2 = \frac{1}{K_2^0} \frac{k_B T}{4d} \frac{L}{d}$ (to avoid the possible role of S) where the coefficient K_2^0 is taken as the value of K_2/S^2 at $T = 294$ K with the experimentally determined $K_2 = 0.65$ pN and the typical $S = 0.7$ [6, 12]. Then with $K_2^0 = 1.32$ pN and $d = 1.6$ nm [13], we use the experimental data for K_1/K_2 to deduce $L_0 = 0.86$ nm, $L(T)$, and E_a (as shown in Fig. 3 d). L decreases from 75 nm at 294 K to 34 nm at 300 K [14], which is consistent with the estimate $L = 18$ nm [10] for the isotropic phase at 305K. Furthermore, the scission energy shows a weak temperature dependency, changing from $E_a = 3.3 \times 10^{-20}$ J at 294K to $E_a = 2.8 \times 10^{-20}$ J at 300K, which amounts to $(7-8)k_B T$, in agreement with estimates for chromonic dyes and DNA oligomers [4, 12].

The case of K_3 is the most difficult to discuss as it might depend not only on L but also on the persistence length P of the aggregates. In the model of rigid rods, $P \rightarrow \infty$, and $K_3/K_1 \propto L/d$ should decrease with increasing T if the aggregates become shorter [11], contrary to the experimentally observed behavior in our chromonematic (Fig. 3 a). The observed increase of K_3/K_1 with T might be consistent with the model of the flexible rods, in which [11] $K_3 \propto P$ is independent of L while $K_1 \propto L$;

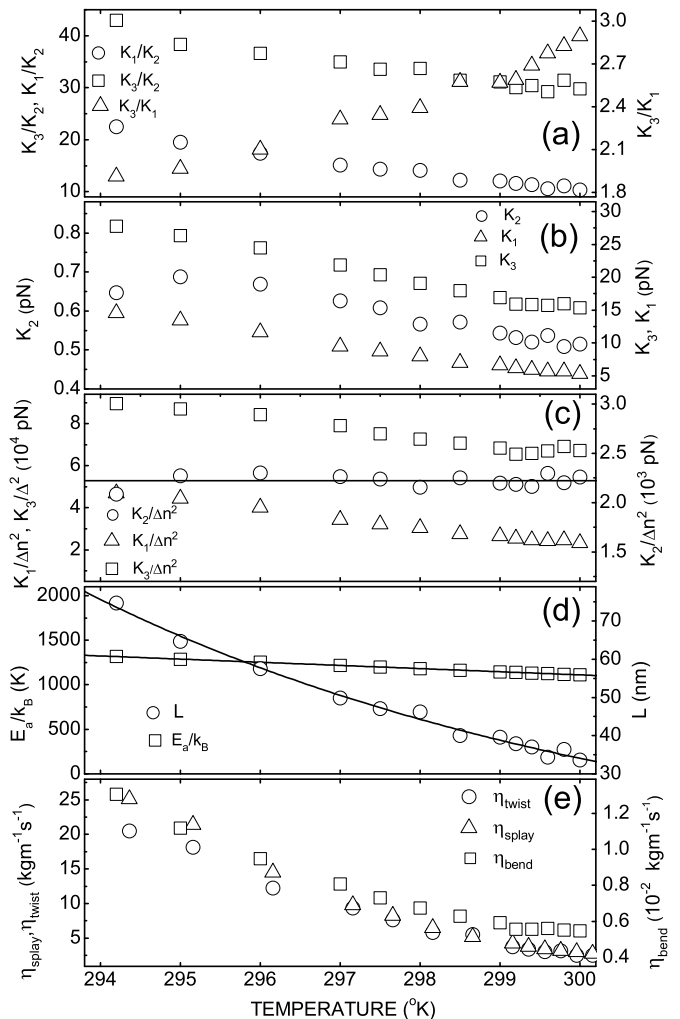


FIG. 3: Temperature dependence of the elastic moduli (a, b), reduced moduli (c), parameters L and E_a (d), and orientational viscosities (e), for the studied chromo-nematic.

however, the data on P are not presently available.

The viscosity coefficients η_{splay} , η_{twist} and η_{bend} all decrease on heating (Fig. 3e), as in other nematics. It is of interest to compare them to the viscosities measured (at room temperatures) for the low-molecular weight 5CB [15], and for the lyotropic polymer nematic poly- γ -benzyl-glutamate (PBG) [5]: η_{bend} (5CB : PBG : DSCG) = $(0.028 : 0.016 : 0.013)$ $\text{kgm}^{-1}\text{s}^{-1}$ and η_{twist} (5CB : PBG : DSCG) = $(0.08 : 3.5 : 20.5)$ $\text{kgm}^{-1}\text{s}^{-1}$. Clearly, η_{bend} in all three systems is of the same order, while η_{twist} in the polymer and chromonematic is two-three orders of magnitude higher than in 5CB. The large ratio of $\eta_{twist}/\eta_{bend} \approx 1600$ measured for DSCG is not unusual from the point of view of the theory [5] and resemble findings for the polymer nematics [16]: η_{bend} for sufficiently extended aggregates is associated mainly with the relatively easy process of sliding of the aggregates along each

other, while η_{twist} should involve rearrangements of the aggregates. Interestingly, η_{twist}/η_{bend} decreases dramatically with T , to ≈ 450 at 300K. Such a behavior can be tentatively explained by the fact that the aggregates become shorter at high T , which should dramatically decrease η_{twist} and less so η_{bend} . It is of interest to explore in the future the role of possible breaking and recombination of chromonic aggregates in the dynamics of LCLCs.

An interesting phenomenon observed in the course of our experiments is the development at a threshold laser power of a strong forward diffraction pattern. Evidently a transformation of the sample structure takes place above the threshold power, which was about 30 mW at $T = 294$ K, and decreased on heating, vanishing near the temperature $T_{NI} = 301$ K. To avoid any significant influence on our results reported above, we kept the laser power as low as feasible between 1.5 and 3 mW and well below the threshold for all T studied. This is also why we do not include in Fig.3 data measured in the vicinity of T_{NI} , which might be affected by the laser power.

It remains to discuss the additional mode $[A_4, \Gamma_4]$ observed in the bend geometry. Since its amplitude is ~ 7 times smaller than the amplitude of the bend mode, its influence, if any, on the results obtained in the bend geometry, is small: K_3 might be slightly overestimated (by less than 15%). Concerning the origin of this mode, we can suggest that it corresponds to the translation diffusion either of monomers, short aggregates ($L \sim d$) or to a transverse sliding of DSCG molecules or their clusters within the overall aggregates. From data for Γ_4 shown in Fig. 2b using Einstein's formula for the diffusion coefficient of spherical scatterers, we find the hydrodynamic diameter $d_h = 3.2$ nm, which is twice the aggregate diameter $d \approx 1.6$ nm [13] and could reflect short aggregates. However the studied system is expected to be poly-disperse in length and it is not likely that only the diffusion of short aggregates would be detected. On the other hand, if we assume that the mode $[A_4, \Gamma_4]$ corresponds to the lateral sliding, we have to account for the drag force from the neighboring molecules. According to ref. [17] this can be done by replacing the solvent viscosity η with the effective viscosity $\eta_{eff} = c\eta$, where the drag coefficient $c \approx 2$ [17]. If we use η_{eff} instead of η , we arrive at $d_h \approx d$. It is thus plausible that the mode $[A_4, \Gamma_4]$ corresponds to the sliding of molecules within the aggregates. This sliding can provide a bending flexibility mechanism for the aggregates that differs from the known bending mechanisms in other rod-like nematics.

To conclude, we have measured for the first time the temperature dependencies of the elastic moduli and corresponding viscosities for a new type of lyotropic nematic, the self-assembled chromonic nematic. The observed anomalous temperature behavior of the splay and bend elastic constants indicates that the system is differ-

ent from the well studied nematic phases of thermotropic low-molecular weight liquid crystals and their lyotropic counterparts formed either by hard rods or flexible filaments. One of the key mechanisms contributing to these differences is the temperature dependence of the average aggregate length. These and other features increasingly point to the chromonematics as a phenomenologically richer system than liquid crystals formed by building units of a fixed size.

This work was supported by NSF Materials World Network on Lyotropic Chromonic Liquid Crystals, grant DMR076290, by Samsung Electronics Corp. and by Fundamental Research State Fund Project UU24/018.

* Electronic address: odl@lci.kent.edu

† Electronic address: ssprunt@kent.edu

- [1] J. Lydon, *Current Opin. Coll. Int. Sci.* 3, 458 (1998).
- [2] P. van der Schoot and M. E. Cates, *Langmuir*, 10, 670 (1994).
- [3] R. B. Meyer, in *Polymer Liquid Crystals*, ed. A. Ciferri, W. R. Krigbaum, and R. B. Meyer (New York, Academic Press, 1982).
- [4] M. Nakata, G. Zanchetta, B. D. Chapman, C. D. Jones, J. O. Cross, R. Pindak, T. Bellini, N. A. Clark, *Science*, 318, 1276 (2007).
- [5] V. G. Taratuta, A. J. Hurd, and R. B. Meyer, *Phys. Rev. Lett.* 55, 246 (1985).
- [6] Yu. A. Nastishin, H. Liu, T. Schneider, V. Nazarenko, R. Vasyuta, S. V. Shiyankovskii, and O. D. Lavrentovich, *Phys. Rev.* E72, 041711 (2005).
- [7] P. G. de Gennes and J. Prost, *The Physics of Liquid Crystals*, 2nd ed. (Oxford, Clarendon Press, 1993).
- [8] S. W. Provencher, *Comput. Phys. Commun.* 27, 213 & 229 (1982).
- [9] P. P. Karat, N. V. Madhusudana, *Mol. Cryst. Liq. Cryst.* 40, 239 (1977).
- [10] Yu. A. Nastishin, H. Liu, S. V. Shiyankovskii, O. D. Lavrentovich, A. F. Kostko, and M. A. Anisimov, *Phys. Rev.* E70, 051706 (2004).
- [11] P. G. de Gennes, in *Polymer Liquid Crystals*, ed. by A. Ciferri, W. R. Krigbaum, and R. B. Meyer (New York, Academic Press, 1982).
- [12] V. R. Horowitz, L. A. Janowitz, A. L. Modic, P. A. Heiney, and P. J. Collings, *Phys. Rev.* E72, 041710 (2005).
- [13] N. H. Hartshorne and G. D. Woodard, *Mol. Cryst. Liq. Cryst.*, 23, 343 (1973).
- [14] The data remain essentially the same when one uses $\frac{K_1}{(\Delta n)^2}$ for analysis. If one uses $K_1(T)$ without S -normalization then the fitted L varies from 39 nm to 13 nm in the same temperature interval.
- [15] M. Cui and J. R. Kelly, *Mol. Cryst. Liq. Cryst.* 331, 49 (1999).
- [16] S. D. Lee and R. B. Meyer, *Liq. Cryst.* 7, 15 (1990).
- [17] G. Li and J. X. Tang, *Phys. Rev.* E69, 061921 (2004).